SCIENCE CHINA
Life Sciences

•RESEARCH PAPER•

September 2018 Vol.61 No.9: 1049–1059
https://doi.org/10.1007/s11427-018-9318-8

Aquaporin 5 is degraded by autophagy in diabetic submandibular gland

Yan Huang[1], Xijin Shi[2], Qianying Mao[1], Yan Zhang[2], Xin Cong[2], Xueming Zhang[1], Zhejing Zhang[2], Liling Wu[2], Ruolan Xiang[2*] & Guangyan Yu[1*]

[1]*Department of Oral and Maxillofacial Surgery, Peking University School and Hospital of Stomatology, Beijing 100081, China;*
[2]*Department of Physiology and Pathophysiology, Peking University School of Basic Medical Sciences, Key Laboratory of Molecular Cardiovascular Sciences, Ministry of Education, and Beijing Key Laboratory of Cardiovascular Receptors Research, Beijing 100191, China*

Received April 26, 2018; accepted May 16, 2018; published online June 26, 2018

Autophagy is a catabolic process which is involved in the development of many diseases including diabetes mellitus and its complications. Hyposalivation is a common complication of diabetes mellitus, whereas its mechanism remains unclear. Here, we observed that the stimulated salivary flow rate of SMG was significantly decreased in db/db mice, a diabetic mice model. The expressions of aquaporin 5 (AQP5), a water channel protein, were decreased, whereas the mRNA level of *AQP5* was increased in SMGs of both diabetic patients and mice. Under transmission electron microcope, more autophagosomes were detected in diabetic SMGs. Expressions of autophagy related proteins LC3II, Beclin-1 and ATG5 were increased, meanwhile autophagy substrate p62 was decreased in SMGs of diabetic patients and mice, indicating that autophagy was activated in diabetic SMG. Double immunofluorescence staining showed that the colocalization of AQP5 and LC3 was increased in SMGs of diabetic mice. In cultured SMG-C6 cells, high glucose (HG), but not high osmotic pressure, reduced AQP5 protein expression and induced autophagy. Moreover, inhibition of autophagy by 3-methyladenin, an autophagy inhibitor, or by autophagy-related gene 5 siRNA, decreased HG-induced AQP5 reduction in SMG-C6 cells. Additionally, the expression of p-p85, p-Akt and p-mTOR were decreased in HG-treated SMG-C6 cells. Pretreatment with 740Y-P, a PI3K agonist, significantly suppressed HG-induced autophagy and AQP5 degradation. Taken together, these results indicate that autophagy plays a crucial role in AQP5 degradation in diabetic SMG via PI3K/Akt/mTOR signaling pathway, which contributes to the dysfunction of diabetic SMG. Our study provides a novel mechanism of diabetic hyposalivation.

diabetes mellitus, submandibular gland, autophagy, aquaporin 5, hyposalivation

Citation: Huang, Y., Shi, X., Mao, Q., Zhang, Y., Cong, X., Zhang, X., Zhang, Z., Wu, L., Xiang, R., and Yu, G. (2018). Aquaporin 5 is degraded by autophagy in diabetic submandibular gland. Sci China Life Sci 61, 1049–1059. https://doi.org/10.1007/s11427-018-9318-8

INTRODUCTION

Diabetes mellitus is characterized by relative or absolute lack of insulin and results in hyperglycemia, which causes long-term damage in diverse organs, including salivary glands (Babu et al., 2014). Impaired functions of salivary glands are found in diabetic patients and lead to decreased oral salivary flow, which consequently triggers a series of oral problems and influences the quality of life (Abd-Elraheem et al., 2017; Mandel, 1989). However, the mechanism of hyposalivation in diabetic patient remains unclarified.

Saliva secretion is mainly accomplished through trans-cellular and paracellular pathways (Proctor and Carpenter, 2014). Aquaporins (AQPs) are a family of water-specific channel proteins that contributes to fast transmembrane water transport. Among the four AQPs (AQP1, AQP4, AQP5 and AQP8) expressed in salivary glands, AQP5 plays

*Corresponding authors (Ruolan Xiang, email: xiangrl@bjmu.edu.cn; Guangyan Yu, email: gyyu@263.net)

a significant role in salivary secretion (Hosoi, 2016). The stimulated salivary flow is decreased more than 50% in AQP5 knockout mice (Krane et al., 2001; Ma et al., 1999). Abnormal distribution of AQP5 in minor salivary glands is observed in Sjögren's syndrome patients (Steinfeld et al., 2001). Therefore, the changes in the expression and distribution of AQP5 can influence salivary secretion in diseases. However, the change of AQP5 in diabetic submandibular gland (SMG) and the related regulatory mechanism remain to be elucidated.

Autophagy is a conserved catabolic process that maintains cellular homeostasis by degrading cellular components, and its dysregulation is implicated in the development of metabolic disorders, including diabetes mellitus and its complications (Li and Le, 2017; Mathiassen et al., 2017; Sridhar et al., 2012). However, the exact role of autophagy in diabetes mellitus is still controversial. In pancreatic β-cells, inhibition of autophagy results in accumulation of amyloid, which induces β-cell death and consequent reduction in insulin secretion as well as impairment of glucose tolerance (Kim et al., 2014). However, in diabetic heart, increased level of autophagy contributes to the deficiency of cardiac function through promoting progressive loss of cardiac cells (Munasinghe et al., 2016). Recently, autophagy is found to be an important degradation pathway in eukaryotic cells. It has been reported that AQP5 was degraded through autophagy pathway in parasympathetic denervation (Azlina et al., 2010). However, whether autophagy is involved in the dysfunction of SMG in diabetes mellitus is still unknown.

Therefore, the present study was designed to explore the changes of AQP5 and autophagy in SMGs of diabetic mice and patients. Furthermore, we investigated the role of autophagy in the dysfunction of diabetic SMG and its regulatory signaling pathway.

RESULTS

Morphology and secretion of SMGs are impaired in diabetic mice

The clinical and biochemical parameters of mice are shown in Table 1. Although the body weight was higher, the weight and size of SMGs were significantly decreased in db/db mice compared with db/m mice (Figure 1A–C). The ratio of gland weight to body weight was markedly reduced in db/db mice (Figure 1D). HE staining exhibited an obvious enlargement of acini and an atrophy of ducts in db/db mice (Figure 1E–G). The area ratio of acini and ducts in each field of view were respectively increased by 56.3% and decreased by 50.8% in db/db mice (Figure 1H and I). Moreover, DMAB staining showed less number of granular convoluted tubules (GCTs) in db/db mice than that in db/m mice (Figure 1J and K). Additionally, an enlargement of acini was also detected in SMGs of diabetic patients (Figure 1L and M). We further investigated the secretory function of SMG in diabetic mice. The stimulated salivary flow rate of SMG was decreased by 80.3% in db/db mice (Figure 1N). The SMG stimulated salivary flow rate normalized by gland weight was also reduced (Figure 1O). The total protein contents of saliva collecting from SMGs were similar between two groups (Figure 1P). These results indicate that the structure and secretory function of SMG are impaired in diabetes mellitus.

Expression of AQP5 protein is decreased in diabetic SMG

To investigate the mechanism in the dysfunction of diabetic SMG, we detected the expression of AQP5, which is a critical molecule in salivary secretion. RT-PCR showed that the mRNA level of *AQP5* was increased in db/db mice (Figure 2A). However, western blot and immunohistochemistry revealed that the protein level of AQP5 was lower in db/db mice (Figure 2B–D). The functional AQP5 is located in apical membrane. In order to estimate secretory function of AQP5, we further extracted protein from membrane and cytoplasmic fracture of mouse SMGs, respectively. Western blot showed that the expression of AQP5 was decreased in apicolateral membrane and increased in acinar cytoplasm of db/db mice when compared with db/m mice, which indicates that the distribution of AQP5 is changed in diabetic mice (Figure 2E and F). The lower expression and redistribution of AQP5 may be responsible for the impaired function of SMG in diabetic mice.

We then examined AQP5 in SMGs of diabetic patients. Results showed that the mRNA level of *AQP5* was higher and the protein level of AQP5 was lower in diabetic patients. AQP5 was predominantly located in the apicolateral membranes of acinar cells in non-diabetic patients; however, more AQP5 was scattered in the acinar cytoplasm in diabetic patients (Figure 2G–J). Quantitative analysis showed that the intensity of AQP5 was decreased by 48.6% in apicolateral membrane, while increased by 38.4% in acinar cytoplasm of diabetic patients (Figure 2K and L). All these results suggest that AQP5 expression and function are decreased in diabetic SMG.

Autophagy is activated in diabetic SMG

To explore the mechanism involved in the reduction of AQP5 in diabetic SMGs, we detected the autophagy level. The expression of LC3-II, an autophagy marker, was significantly increased in db/db mice compared to db/m mice (Figure 3A and B). In addition, the expressions of autophagy-related proteins, including Beclin-1 and ATG5, were markedly increased, whereas the expression of p62, an autophagy substrate, was significantly reduced in db/db mice

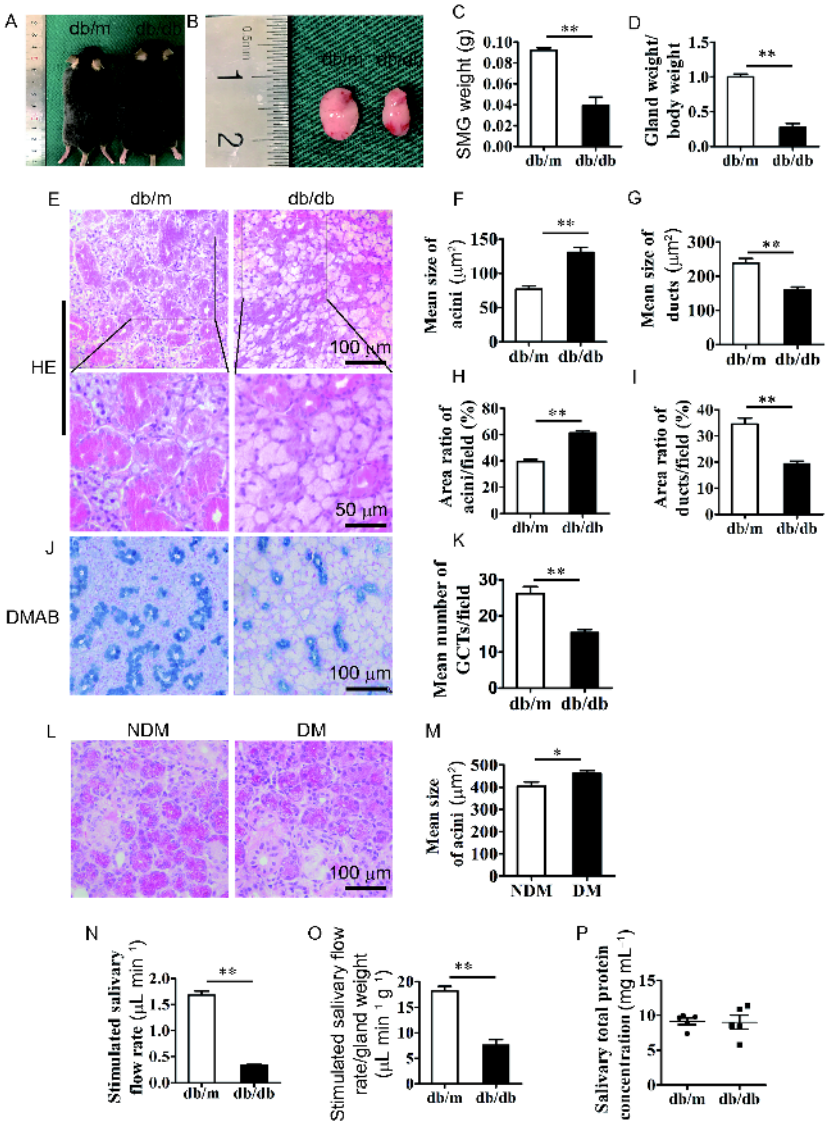

Figure 1 Morphology and secretion of SMGs are impaired in diabetic mice. A, The picture of db/m and db/db mice. B, The picture of SMGs from db/m and db/db mice. C, The weight of SMG. D, The ratio of SMG weight to body weigt. E, Hematoxylin-eosin (HE) staining of SMGs from db/m and db/db mice. Scale bars, 100 and 50 μm. F and G, Mean size of acini and ducts. H and I, Mean area ratio of acini and duct in each field of view. J, DMAB staining of SMGs from db/m and db/db mice. Scale bars, 100 μm. K, The mean number of granular convoluted tubules (GCTs) in each field of view. L, HE staining of human SMGs. M, Mean size of acini in human SMGs. N, The pilocarpine (10 μg g^{-1})-stimulated, gland-specific salivary flow rates (μL min^{-1}) of SMGs in db/m and db/db mice. O, Normalized stimulated salivary flow rate by gland weight (μL min^{-1} g^{-1}). P, The total protein concentration of saliva collected from SMGs in db/m and db/db mice. Data are presented as mean±SE. n=5–6, *, P<0.05 and **, P<0.01. NDM, non-diabetic patients; DM, diabetic patients.

Table 1 The clinical and biochemical parameters of mice[a)]

Group	Body weight (g)	Food intake (g day^{-1})	Water intake (mL day^{-1})	Blood glucose (mmol L^{-1})	Serum insulin (mU L^{-1})
db/m	34.72±2.96	3.47±0.18	7.5±1.37	7.18±0.68	12.98±4.78
db/db	53.73±8.38**	4.89±0.44**	13.2±1.1**	25.52±2.15**	22.31±3.67*

a) Mean±SE, n=6, *, P<0.05; **, P<0.01, vs. db/m.

(Figure 3C–E). Under transmission electron microcope, more autophagosomes were observed in db/db mice (Figure 3F). Double immunofluorescence staining showed increased number of LC3 (autophagosome marker) and Lamp2 (lysosome marker) positive dots in SMGs of db/db mice (Figure 3G). These results indicate that autophagy is activated in SMGs of db/db mice.

Consistent with the results in db/db mice, more autophagosomes were observed in SMGs of diabetic patients (Figure 3H). LC3-II and Beclin-1 expressions were higher and p62

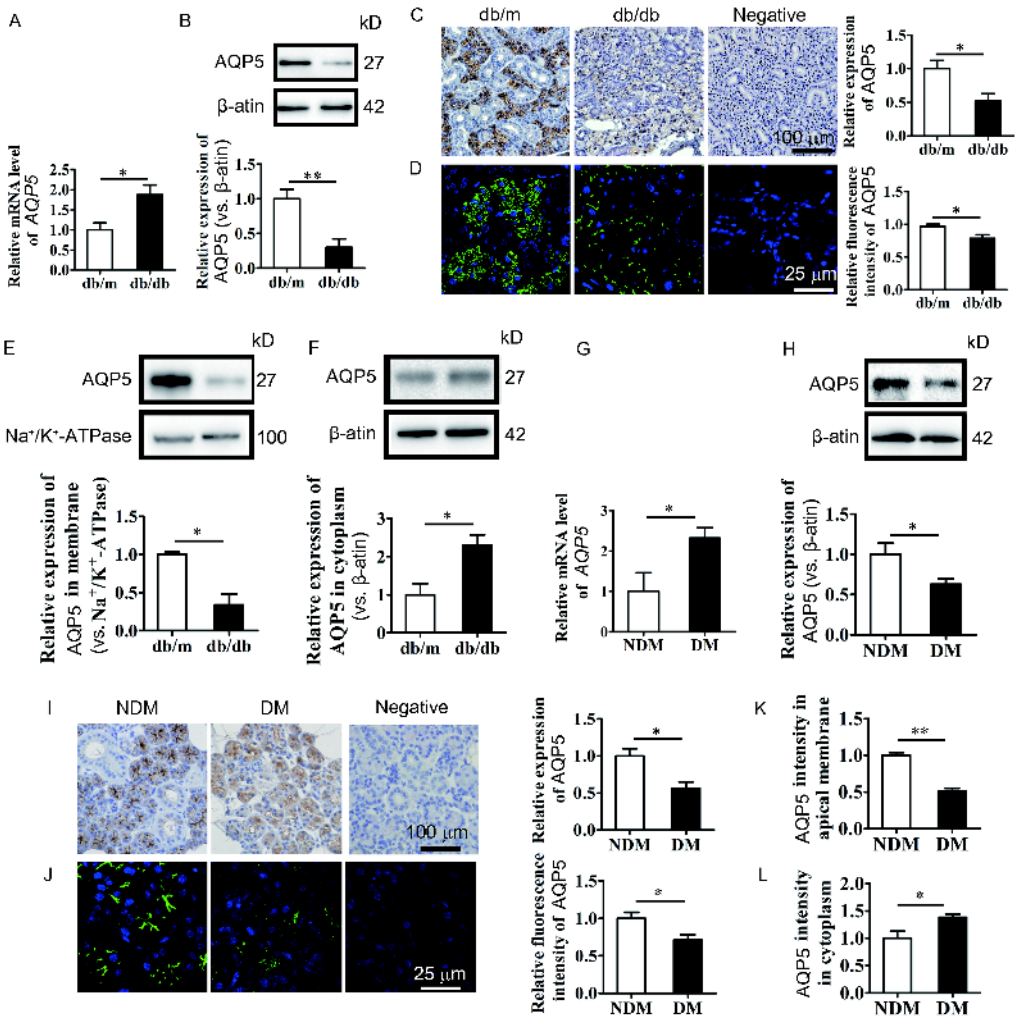

Figure 2 Expression of AQP5 protein is decreased in diabetic SMG. A, The mRNA expression of *AQP5* in mice SMGs. B, Western blot analysis of AQP5 in SMGs from db/m and db/db mice. C and D, Immunohistochemistry and immunofluorescence staining of AQP5 in SMGs of db/m and db/db mice. E and F, Western blot analysis of AQP5 in membrane and cytoplasm of mice SMGs. G, The mRNA expression of *AQP5* in human SMGs. H, Western blot analysis of AQP5 in human SMGs. I and J, Immunohistochemistry and immunofluorescence staining of AQP5 in human SMGs. K, AQP5 intensity in apicolateral membrane of human SMGs. L, AQP5 intensity in acinar cytoplasm of human SMGs. Data are presented as mean±SE. n=5–6, *, P<0.05 and **, P<0.01. Scale bars, 100 and 25 μm. NDM, non-diabetic patients; DM, diabetic patients.

expression was lower in SMGs of diabetic patients compared with non-diabetic patients (Figure 3I–L). These results suggest that autophagy is activated in SMGs of diabetic patients.

Activated autophagy is responsible for AQP5 reduction in diabetic SMG

To explore whether the activated autophagy is related with AQP5 reduction in diabetic SMG, we examined the colocalization of AQP5 and LC3. More autophagosome-like structures with positive staining for both AQP5 and LC3 were observed in SMGs of db/db mice and diabetic patients (Figure 3M and N), indicating that autophagy might participate in the reduction of AQP5 in diabetic SMG.

To detect the direct relationship between autophagy and AQP5, we incubated SMG-C6 cells with the medium containing 25 mmol L^{-1} high glucose (HG) for 12 h. Mannitol (25 mmol L^{-1}) was used as osmotic control. Consistently, AQP5 protein expression was decreased in HG group compared with normal glucose (NG) group, but not in mannitol group (Figure 4A). These results suggested that HG directly reduced the protein level of AQP5 in SMG-C6 cells. We then detected the autophagy level in HG-treated SMG-C6 cells. Rapamycin (1 ng mL^{-1}), an autophagy inducer, was used as a positive control. Immunofluorescence image exhibited that more colocalization dots positive for both Lamp2 and LC3 were detected in HG and rapamycin groups (Figure 4B). Western blot further showed the up-regulation of LC3II, Beclin-1 and ATG5 in HG and rapamycin groups. These results indicate that HG can directly induce autophagy in SMG-C6 cells (Figure 4C–F).

Furthermore, we inhibited autophagy by 3-methyladenin

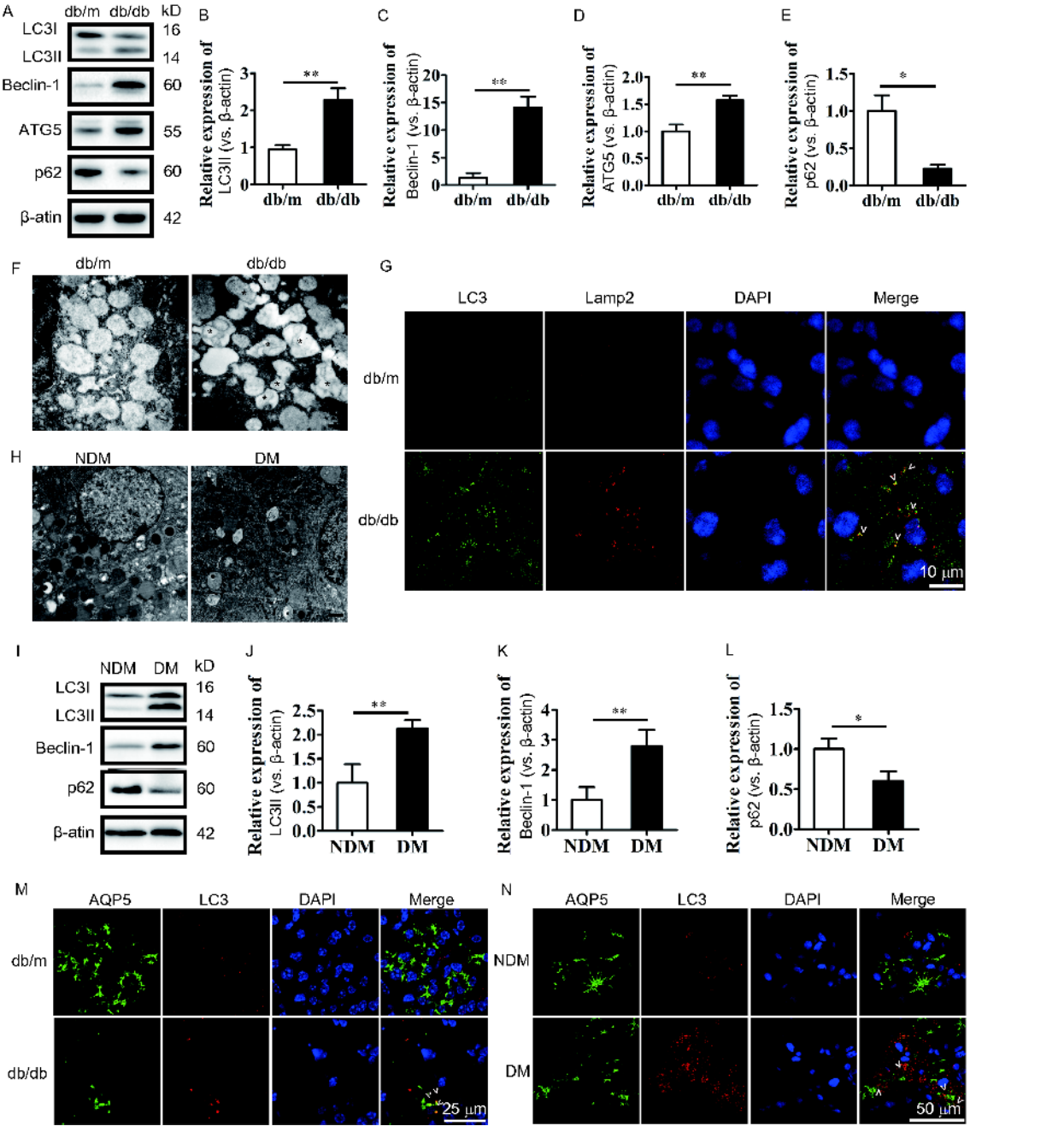

Figure 3 Autophagy is activated in diabetic SMG. A–E, Western blot analysis of LC3, Beclin-1, ATG5, p62 in SMGs of db/m and db/db mice. F, Transmission electron microscopy images of SMGs from db/m and db/db mice. Note the autophagosome-like structure (black star). Scale bars, 500 nm. G, Double immunofluorescent assay for LC3 (green dots) and Lamp2 (red dots) in SMGs of db/m and db/db mice. Note the autolysosome-like structure (yellow dots). Scale bars, 10 μm. H, Transmission electron microscopy images of SMGs from non-diabetic patients and diabetic patients. Note the autophagosome-like structure (white star). Scale bars, 1 μm. I–L, Western blot analysis of LC3, Beclin-1 and p62 of SMGs from non-diabetic patients and diabetic patients. M and N, Double immunofluorescent assay for AQP5 (green dots) and LC3 (red dots) in SMGs of mice and patients. Scale bars, 25 μm. Data are presented as mean±SE. n=5–6, *, P<0.05 and **, P<0.01. NDM, non-diabetic patients; DM, diabetic patients.

(3-MA, 1 mmol L^{-1}) in SMG-C6 cells, and found that the HG-induced AQP5 reduction was reversed (Figure 4G–I). Additionally, *ATG5* siRNA was effective as identified by both RT-PCR and western blot (Figure 4J–L). After inhibition of autophagy by *ATG5* siRNA, the HG-induced AQP5 reduction was also rescued (Figure 4M–P). These above data suggest that the activated autophagy is responsible for AQP5 reduction in diabetic SMG.

HG induces autophagic degradation of AQP5 through PI3K/Akt/mTOR pathway

We next investigated the possible molecular mechanism of HG-induced autophagic degradation of AQP5. PI3K/Akt/

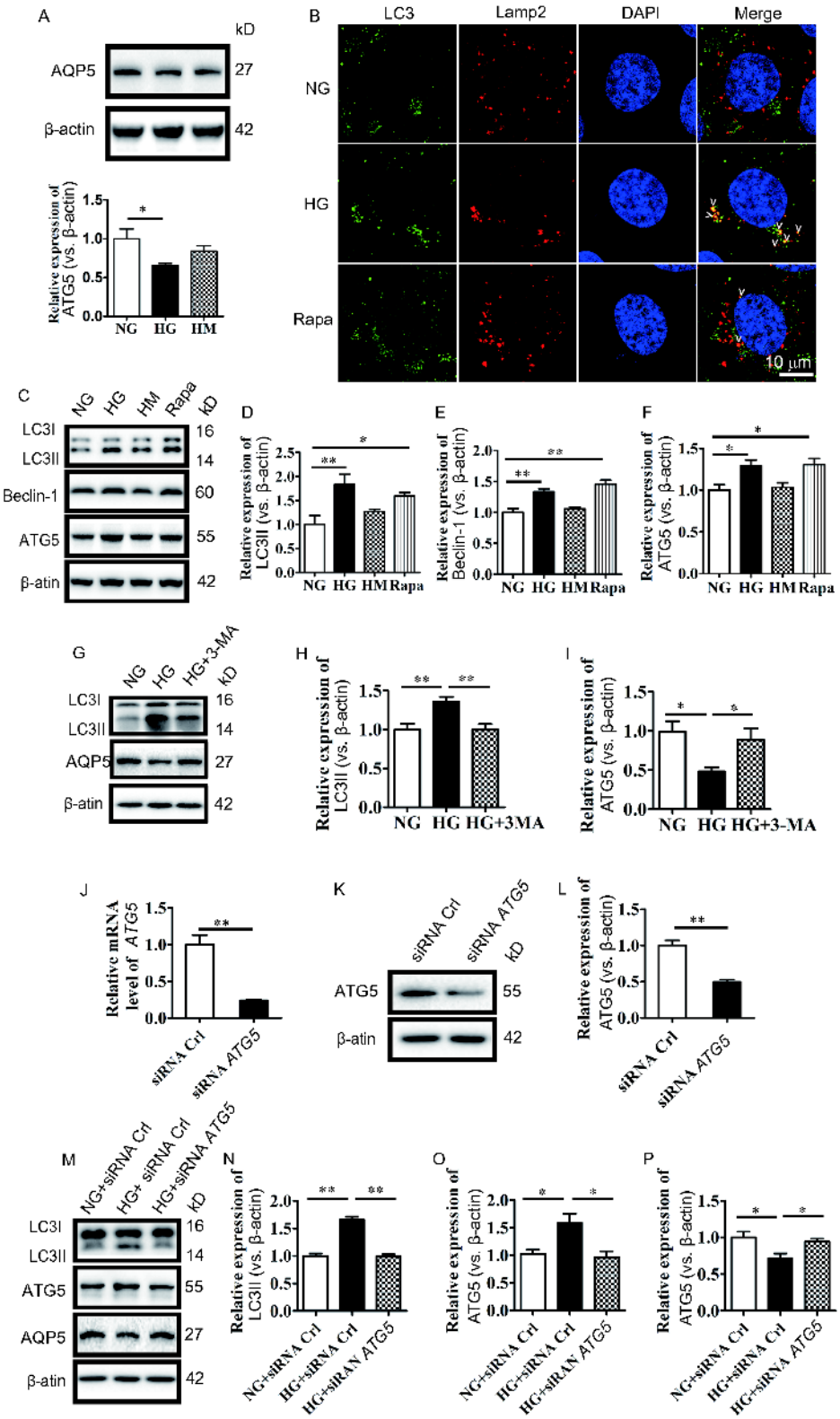

Figure 4 Activated autophagy is responsible for AQP5 reduction in diabetic SMG. A, Western blot analysis of AQP5 from SMG-C6 cells cultured in medium containing normal glucose (NG), high glucose (HG) and high mannitol (HM). *n*=3. B, Double immunofluorescent assay for LC3 (green dots) and Lamp2 (red dots) in NG, HG and rapamycin (Rapa) treated SMG-C6 cells. Scale bars, 10 μm. C–F, Western blot analysis of LC3, Beclin-1 and ATG5 in NG, HG, HM and Rapa treated SMG-C6 cells. *n*=4. G–I, Western blot analysis of LC3 and AQP5 from SMG-C6 cells cultured in medium containing normal glucose (NG), high glucose (HG) and HG+3-MA (1 mmol/L). *n*=5. J–L, Knocking down *ATG5* in SMG-C6 cells by transfecting with *ATG5* siRNA. *n*=3. M–P, Transfecting SMG-C6 cells with control (Crl) siRNA and *ATG5* siRNA, then the cells were incubated in NG and HG medium, the expression of LC3, ATG5 and AQP5 were detected by Western blot. *n*=5. Data are presented as mean±SE. *, $P<0.05$ and **, $P<0.01$.

mTOR signaling pathway is one of the major regulatory pathways of autophagy. HG significantly reduced the phosphorylation of p85, a regulatory subunit of PI3K, Akt and mTOR (Figure 5A–C). However, preincubation with PI3K agonist 740Y-P (50 μg mL^{-1}, 1 h) enhanced the phosphorylation of p85, Akt and mTOR in HG condition (Figure 5D–F), and significantly suppressed HG-induced up-regulation of autophagy and down-regulation of AQP5 in SMG-C6 cells (Figure 5G and H). The data indicate that PI3K/Akt/mTOR signaling pathway is involved in HG-induced autophagy and AQP5 degradation.

DISCUSSION

In the present study, we demonstrated that secretion of SMG was impaired in diabetic mice. Autophagy was activated in SMGs of both diabetic patients and mice, which contributed to the dysfunction of diabetic SMG by excessively degrading AQP5. Furthermore, the PI3K/Akt/mTOR signaling pathway was involved in HG-induced autophagic degradation of AQP5. Our study provides new insights into the mechanism of diabetic hyposalivation.

Diabetes mellitus can severely affect oral health, and common complications such as dry mouth, caries, periodontal disease and infections, are largely due to inadequate saliva in diabetic patients (Chuang et al., 2005; Xiao et al., 2017). In human, about 60% of resting saliva and 40% of stimulated saliva are secreted from SMG (Garrett, 1987). However, studies focusing on the changes of diabetic SMG and its underlying mechanism are very limited. It has been reported that a significant enlargement of acini and secretory granule size in SMGs of diabetic patients (Lilliu et al., 2015). High prevalence of reduced salivary flow rate is also observed among diabetic patients. Clinical study shows that 92.5% older patients with type 2 diabetes mellitus experience decreased salivary flow rate (Lima et al., 2017). In the present study, we observed an atrophy of SMGs in db/db mice. Histological staining exhibited an obvious enlargement of acini and an atrophy of ducts in db/db mice compared to db/m mice. Additionally, the size of acini was also enlarged in diabetic patients. Moreover, the stimulated salivary flow rate of SMG detected by SMG intubation was significantly reduced in db/db mice. These results indicate that morphology and function of SMG are impaired in diabetes mellitus.

AQP5 plays a significant role in rapid water movement across the plasma membrane in SMG. Many studies indicate that down-regulation and abnormal distribution of AQP5 in salivary glands are responsible for disease-related xerostomia, such as Sjögren's syndrome, radiation and inflammation (Alam et al., 2017; Li et al., 2006; Murdiastuti et al., 2006; Steinfeld et al., 2001). However, the exact mechanism in modulating the expression and distribution of AQP5 in diabetic SMG is still unknown. In the present study, although the mRNA level of *AQP5* was up-regulated, its protein level was markedly reduced in SMGs of both diabetic patients and mice. Moreover, HG directly inhibited the expression of AQP5 protein in SMG-C6 cells. Our results confirmed that the level of AQP5 protein was decreased *in vivo* and *in vitro*. The abnormal distribution of AQP5 from the cell membrane into the cytoplasm triggered by various stimuli is closely associated with pathological water movement (Xu et al., 2015). In the present study, the redistribution of AQP5 from the apicolateral membrane into cytoplasm was observed in SMG acinar cells in diabetic mice and patients, which suggests that the functional AQP5 is decreased in diabetic SMG. Both reduced expression and redistribution of AQP5 contribute to the dysfunction of diabetic SMG.

Recently, investigations have found that autophagy is involved in the pathological process of diabetes mellitus and its complications (Jung and Lee, 2010; Yang et al., 2017). In β-cells, autophagy degrades proinsulin and insulin, and inhibition of autophagy can increase insulin secretion (Riahi et al., 2016). Moreover, augmented autophagy level is detected in the diabetic heart, skeletal muscle, kidney and liver (Liu et al., 2016; Munasinghe et al., 2016; Robinson et al., 2016; Yao et al., 2016). The development and secretory capacity of salivary glands are also reported to be critically intertwined with autophagy (Morgan-Bathke et al., 2015). However, little is known about the changes and role of autophagy in diabetic SMG. Here, we observed more autophgosomes and found up-regulation of autophagy marker LC3II, as well as down-regulation of autophagy substrate p62 in SMGs of both db/db mice and diabetic patients. Beclin-1 is the mammalian homolog of yeast Atg 6 and plays a critical role in the regulation of autophagy. It is regulated by molecules such as advanced glycation end products, which have been demonstrated to be increased in diabetes mellitus (Sinha and Levine, 2008). Moreover, diabetes can inhibit mTOR signaling pathways which induces activation of Beclin-1 (Munasinghe et al., 2016). ATG5 is also a key regulator of autophagy, which is responsible for elongation of the phagophore in the autophagy process by conjugated to ATG12. Many protein kinases can regulate activity of ATG5 including PI3K/Akt pathway (Yin et al., 2016). Additionally, ATG5 is demonstrated to be up-regulated in HG condition (Kong et al., 2014; Liu et al., 2014; Ma et al., 2013). Therefore, we also detected Beclin-1 and ATG5 to evaluate autophagy level. The expression of Beclin-1 and ATG5 were also increased in diabetic SMG. Additionally, the colocalization of autophagosome marker LC3 and lysosome marker Lamp2 was increased in db/db mice. All these results demonstrate that autophagy is activated in diabetic SMG.

Furthermore, we explored the mechanism of decreased AQP5 in diabetic SMG. The higher mRNA level and lower protein level of AQP5 in diabetic SMG suggested that de-

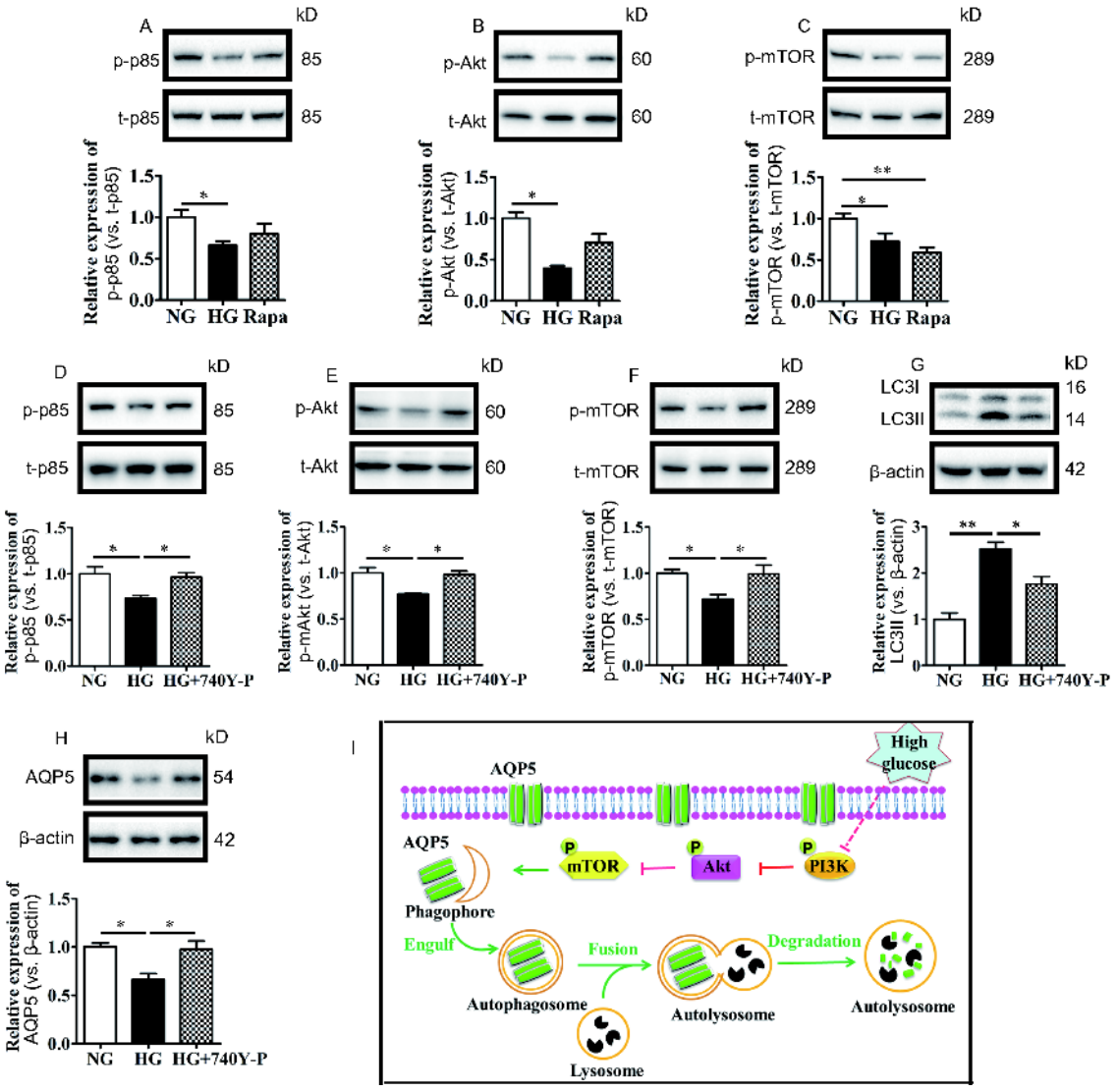

Figure 5 HG induces autophagic degradation of AQP5 through PI3K/Akt/mTOR pathway. A–C, Western blot analysis of p-p85, p-Akt, p-mTOR of SMG-C6 cells cultured in medium containing normal glucose (NG) and high glucose (HG). *n*=4. D–H, Preincubating SMG-C6 cells with PI3K agonist 740Y-P (50 μg mL^{-1},1 h), the expression of p-p85, p-Akt, p-mTOR, LC3 and AQP5 were detected by western blot. *n*=3–6. I, Schematic illustration showing the process of HG-induced autophagic degradation of AQP5 mediated through PI3K/Akt/mTOR signaling pathway in the acinar cells of diabetic SMG. Data are presented as mean±SE. *, P<0.05 and **, P<0.01.

creased AQP5 protein might be due to an elevation in AQP5 degradation. Recently, autophagy has been reported to be an important protein degradation pathway involved in AQP5 degradation. The G103D point mutation of *AQP5* gene in rat SMG causes an increase of autophagy-lysosome degradation of AQP5 (Karabasil et al., 2011). Parasympathetic denervation of the chorda tympani in rat SMG causes a decrease in AQP5 protein level via autophagy-lysosome degradation system (Azlina et al., 2010). Here, we found that more co-localization of AQP5 and LC3 in SMGs of db/db mice. In SMG-C6 cells, HG could directly induce autophagy. Moreover, inhibition of autophagy by 3-MA or *ATG5* siRNA reversed HG-induced AQP5 decrease. Combining *in vivo* and *in vitro* studies, we reveal that autophagic degradation pathway is responsible for decreased AQP5 in diabetic SMG.

The intracellular signaling pathway under HG-induced autophagy was further explored. mTOR is a major negative regulator of autophagy which modulated by several upstream molecules, including PI3K/Akt and adenosine 5′-monophosphate-activated protein kinase (AMPK) (Abada and Elazar, 2014). In diabetic kidney, PI3K/Akt/mTOR pathway is reported to participate in the regulation of autophagy (Huang et al., 2016). In MC3T3-E1 cells, HG increases the production of reactive oxygen species, which induces autophagy through inhibition of Akt/mTOR pathway (Wang et al., 2016). However, whether mTOR was involved in HG-induced autophagic degradation of AQP5 in diabetic SMG is still unclear. Here, the expression of p-mTOR and its up-

stream signals p-p85 and p-Akt were decreased in HG-treated SMG-C6 cells. After activation of PI3K/Akt/mTOR signaling pathway by PI3K agonist, the HG-induced autophagy and AQP5 decrease were inhibited in SMG-C6 cells. These results indicate that HG induces autophagy in diabetic SMG through inhibiting PI3K/Akt/mTOR signaling pathway, while the elevated autophagy excessively degrades AQP5 and leads to the dysfunction of SMG.

In summary, we demonstrate that autophagy plays a crucial role in HG-modulated AQP5 degradation, which contributes to the dysfunction of diabetic SMG. Furthermore, the PI3K/Akt/mTOR signaling pathway is involved in HG-induced autophagic degradation of AQP5. These findings highlight the pathological role and regulatory mechanism of autophagy in diabetic SMG and provide potential target for therapeutic strategy to ameliorate SMG dysfunction in diabetic mellitus.

MATERIALS AND METHODS

Animals

16-week-old male leptin receptor-deficient db/db mice (a model of spontaneous type 2 diabetes mellitus) and age-matched db/m mice were purchased from Changzhou Cavens Laboratory Animal Ltd. The experimental procedure was approved by the Ethics Committee of Animal Research, Peking University Health Science Center and complied with the Guide for the Care and Use of Laboratory Animals (NIH Publication No. 85-23, revised 1996). All animal research is reported in accordance with the ARRIVE guidelines (Kilkenny et al., 2010). Blood samples were collected from the tail veins, the levels of blood glucose and serum insulin were measured by Glucometer (ACCU-CHEK) and Iodine [^{125}I]-Insulin Radioimmunoassay Kit (Union Medical & Pharmaceutical Technology Ltd., Tianjin), respectively.

Human samples

Human SMG samples were collected from five diabetic patients (40 to 70 years old; two males and three females) and five non-diabetic patients (40 to 70 years old; two males and three females) who underwent functional neck dissection for primary oral squamous cell carcinoma without irradiation or chemotherapy. All samples were confirmed to be histologically normal. The research protocol was approved by the Ethics Committee of Peking University Hospital of Stomatology, and all participants had signed an informed consent document before tissue collection.

Cell culture

The rat SMG cell line SMG-C6 was cultured as previously described (Cong et al., 2015). The plasmid containing *AQP5* cDNA (OriGene Technologies, USA) was transfected into the cells by Lipofectamine® 2000 (Thermo Fisher Scientific, USA). At 24 h post-transfection, the cells were subjected to antibiotic G418 (1 mg mL^{-1}; TransGen Biotech, USA) to select the stably overexpressed cells. The independent clones were isolated and passaged.

Measurement of stimulated salivary flow of SMG

Mice were fasted for a minimum of 5 h with water ad libitum. After anesthesia with an intraperitoneal injection of chloral hydrate (0.4 g kg^{-1} body weight), SMG duct was isolated and inserted into a capillary tube. The volume of saliva was measured for 10 min after injection of pilocarpine (10 μg g^{-1} body weight). Total protein content of SMG saliva was detected by using BCA Protein Assay Kit (M&C Gene Technology, USA).

Histological and immunohistochemical staining

Five μm consecutive paraffin sections of SMG were stained with hematoxylin-eosin (HE). Granular ductal kallikreins of SMG were stained by p-dimethylaminobenzaldehyde (DMAB) staining. The morphological changes were observed under a light microscope (Q550CW; Leica). SMG sections were incubated with primary antibody to AQP5 (1:100; Santa Cruz, USA) at 4°C overnight followed by HRP-conjugated secondary antibody (Zhongshan Laboratories). Six fields of each section were randomly chosen to evaluate the morphology of SMG and the intensity of AQP5 by using ImageJ software (National Institutes of Health).

Immunofluorescence staining

Seven μm frozen SMG sections and cells were fixed in cold acetone, stained with primary antibodies to AQP5 (1:100; Santa Cruz), Lysosome-associated membrane protein 2 (Lamp2; 1:100; Santa Cruz) or microtubule-associated protein 1 light chain 3 (LC3; 1:400; Cell Signal Technology, USA) at 4°C overnight, and then incubated with secondary antibodies at 37°C for 2 h. Nuclei were stained with 4,6-diamidino-2-phenylindole (DAPI). Fluorescence images were captured with a confocal microscope (TCS SP8; Leica, Germany). The fluorescent intensities were measured by ImageJ software.

Transmission electron microcopy

SMG tissues were fixed in 2% paraformaldehyde-1.25% glutaraldehyde and stained with uranyl acetate and lead citrate. SMG specimens were examined with a transmission electron microscope (H-7000, HITACHI, Japan).

Table 2 Primers for *AQP5* and *GAPDH* mRNA

Species	Gene	Forward primer (5′→3′)	Reverse primer (5′→3′)
Mouse	*AQP5*	GGCTTTGGCACATGAGATACT	CTTTGGAATTAGGCAGAACGA
Mouse	*GAPDH*	AAATGGTGAAGGTCGGTGTGAA	CAACAATCTCCACTTTGCCACTG
Human	*AQP5*	ACCTTGTCGGAATCTACTTCACT	ACGCTCACTCAGGCTCAG
Human	*GAPDH*	ACATCATCCCTGCCTCTACTG	CCTGCTTCACCACCTTCTTG

Real-time PCR

Total RNA of SMG was extracted and cDNA was synthesized. The primer sequences of *AQP5* and *GAPDH* were listed in Table 2. Real-time PCR (RT-PCR) was carried out with DyNAmo Color Flash SYBR Green qPCR Kit (Thermo Fisher Scientific) according to the manufacturer's instructions.

Western blot

Total proteins of SMGs and SMG-C6 cells were extracted by RIPA lysis buffer. The membrane, cytoplasmic and nuclear proteins were extracted from SMGs by using the Nuclear-Cytosol-Mem Extraction kit (Applygen Technologies Inc., Beijing) following the manufacturer's instructions. Protein concentrations were detected by a BCA Protein Assay Kit (M&C Gene Technology). Same amount of protein was separated on 10% or 12% SDS-PAGE, transferred to polyvinylidene difluoride membrane and probed with primary antibodies to AQP5 (1:1,000; Merck Millipore, USA), Na^+-K^+-ATPase (1:1,000; Ptoteintech, USA), LC3, Beclin-1, SQSTM1/p62, Phosphoinositide 3-kinase (PI3K) p85, phospho-PI3K p85, Akt, phospho-Akt, the mammalian target of rapamycine (mTOR), phospho-mTOR (all 1:1,000; Cell Signal Technology), ATG5 (1:1,000; Bioworld Technology, USA) and β-actin (1:4,000; Abcam, USA) at 4°C overnight, and then incubated with horseradish-peroxidase-conjugated secondary antibodies. Immunoreactive bands were visualized with enhanced chemiluminescence reagent (Thermo Fisher Scientific). The densities of bands were quantified with ImageJ Software.

Knockdown of *ATG5*

SMG-C6 cells were transfected with siRNA using Lipofectamine® RNAiMAX reagent (Thermo Fisher Scientific) according to the manufacturer's instruction. The primer sequence of *ATG5* siRNA was forward 5′-CACUUUAUGUCAUGUGUGAdTdT-3′, reverse 5′-UCACACAUGACAUAAAGUGdTdT-3′, and non-specific negative control siRNA was forward 5′-UUCUCCGAACGUGUCACGUTT-3′, reverse 5′-ACGUGACACGUUCGGAGAATT-3′ (Sigma-Aldrich, USA).

Statistical analysis

Data are presented as mean±SE. Statistical analysis was performed with unpaired Student's *t* test for two groups and one-way ANOVA followed by Bonferroni's test for multiple groups by GraphPad Prism 5.0 software (GraphPad Prism). $P<0.05$ was considered statistically significant.

Compliance and ethics *The author(s) declare that they have no conflict of interest. All procedures performed in studies involving human participants were in accordance with the ethical standards of the institutional and/or national research committee and with the 1964 Helsinki declaration and its later amendments or comparable ethical standards.*

Acknowledgements *We thank Dr. David O. Quissell (University of Colorado Health Science Center, USA) for the generous gift of rat SMG-C6 cell line. We would like to thank Jiazeng Su, Wenxuan Zhu, Kefu Zhang, Yanyan Zhang for their work in the collection of patients' information. This work was supported by National Natural Science Foundation of China (81570993, 81671005) and Beijing Natural Science Foundation of China (7162100).*

Abada, A., and Elazar, Z. (2014). Getting ready for building: signaling and autophagosome biogenesis. EMBO Rep 15, 839–852.
Abd-Elraheem, S.E., El Saeed, A.M., and Mansour, H.H. (2017). Salivary changes in type 2 diabetic patients. Diabetes Metab Syndrome Clin Res Rev 11, S637–S641.
Alam, J., Koh, J.H., Kwok, S.K., Park, S.H., Park, K., and Choi, Y. (2017). Functional epitopes for anti-aquaporin 5 antibodies in Sjögren syndrome. J Dent Res 96, 1414–1421.
Azlina, A., Javkhlan, P., Hiroshima, Y., Hasegawa, T., Yao, C., Akamatsu, T., and Hosoi, K. (2010). Roles of lysosomal proteolytic systems in AQP5 degradation in the submandibular gland of rats following chorda tympani parasympathetic denervation. Am J Physiol Gastrointestinal Liver Physiol 299, G1106–G1117.
Babu, N., Masthan, K., Bhattacharjee, T., and Elumalai, M. (2014). Saliva-the key regulator of oral changes in diabetes patients. Int J Pharmaceut Sci Res 5, 2579–2583.
Chuang, S.F., Sung, J.M., Kuo, S.C., Huang, J.J., and Lee, S.Y. (2005). Oral and dental manifestations in diabetic and nondiabetic uremic patients receiving hemodialysis. Oral Surgery Oral Med Oral Pathol Oral Rad Endodontol 99, 689–695.
Cong, X., Zhang, Y., Li, J., Mei, M., Ding, C., Xiang, R.L., Zhang, L.W., Wang, Y., Wu, L.L., and Yu, G.Y. (2015). Claudin-4 is required for modulation of paracellular permeability by muscarinic acetylcholine receptor in epithelial cells. J Cell Sci 128, 2271–2286.
Garrett, J.R. (1987). The proper role of nerves in salivary secretion: a review. J Dent Res 66, 387–397.
Hosoi, K. (2016). Physiological role of aquaporin 5 in salivary glands. Pflugers Arch 468, 519–539.
Huang, C., Lin, M.Z., Cheng, D., Braet, F., Pollock, C.A., and Chen, X.M. (2016). KCa3.1 mediates dysfunction of tubular autophagy in diabetic kidneys via PI3k/Akt/mTOR signaling pathways. Sci Rep 6, 23884.

Jung, H.S., and Lee, M.S. (2010). Role of autophagy in diabetes and mitochondria. Ann New York Acad Sci 1201, 79–83.
Karabasil, M.R., Hasegawa, T., Azlina, A., Purwanti, N., Yao, C., Akamatsu, T., Tomioka, S., and Hosoi, K. (2011). Effects of naturally occurring G103D point mutation of AQP5 on its water permeability, trafficking and cellular localization in the submandibular gland of rats. Biol Cell 103, 69–86.
Kilkenny, C., Browne, W., Cuthill, I.C., Emerson, M., Altman, D.G., and Altman, D.G. (2010). Animal research: reporting *in vivo* experiments: The ARRIVE guidelines. Br J Pharmacol 160, 1577–1579.
Kim, J., Cheon, H., Jeong, Y.T., Quan, W., Kim, K.H., Cho, J.M., Lim, Y. M., Oh, S.H., Jin, S.M., Kim, J.H., et al. (2014). Amyloidogenic peptide oligomer accumulation in autophagy-deficient β cells induces diabetes. J Clin Invest 124, 3311–3324.
Kong, C.G., Park, J.B., Kim, M.S., and Park, E.Y. (2014). High glucose accelerates autophagy in adult rat intervertebral disc cells. Asian Spine J 8, 543–548.
Krane, C.M., Melvin, J.E., Nguyen, H.V., Richardson, L., Towne, J.E., Doetschman, T., and Menon, A.G. (2001). Salivary acinar cells from aquaporin 5-deficient mice have decreased membrane water permeability and altered cell volume regulation. J Biol Chem 276, 23413–23420.
Li, S., and Le, W. (2017). An insight review of autophagy biology and neurodegenerative diseases: machinery, mechanisms and regulation. Sci China Life Sci 60, 1457–1459.
Li, Z., Zhao, D., Gong, B., Xu, Y., Sun, H., Yang, B., and Zhao, X. (2006). Decreased saliva secretion and down-regulation of AQP5 in submandibular gland in irradiated rats. Radiat Res 165, 678–687.
Lilliu, M.A., Solinas, P., Cossu, M., Puxeddu, R., Loy, F., Isola, R., Quartu, M., Melis, T., and Isola, M. (2015). Diabetes causes morphological changes in human submandibular gland: a morphometric study. J Oral Pathol Med 44, 291–295.
Lima, D.L.F., Carneiro, S.D.R.M., Barbosa, F.T.S., Saintrain, M.V.L., Moizan, J.A.H., and Doucet, J. (2017). Salivary flow and xerostomia in older patients with type 2 diabetes mellitus. PLoS ONE 12, e0180891.
Liu, J., Tang, Y., Feng, Z., Hou, C., Wang, H., Yan, J., Liu, J., Shen, W., Zang, W., Liu, J., et al. (2014). Acetylated FoxO1 mediates high-glucose induced autophagy in H9c2 cardiomyoblasts: regulation by a polyphenol -(−)-epigallocatechin-3-gallate. Metabolism 63, 1314–1323.
Liu, N., Shi, Y., and Zhuang, S. (2016). Autophagy in chronic kidney diseases. Kidney Dis 2, 37–45.
Ma, T., Song, Y., Gillespie, A., Carlson, E.J., Epstein, C.J., and Verkman, A.S. (1999). Defective secretion of saliva in transgenic mice lacking aquaporin-5 water channels. J Biol Chem 274, 20071–20074.
Ma, T., Zhu, J., Chen, X., Zha, D., Singhal, P.C., and Ding, G. (2013). High glucose induces autophagy in podocytes. Exp Cell Res 319, 779–789.
Mandel, I.D. (1989). The role of saliva in maintaining oral homeostasis. J Am Dent Assoc 119, 298–304.
Mathiassen, S.G., De Zio, D., and Cecconi, F. (2017). Autophagy and the cell cycle: a complex landscape. Front Oncol 7, 51.
Morgan-Bathke, M., Lin, H.H., Ann, D.K., and Limesand, K.H. (2015). The role of autophagy in salivary gland homeostasis and stress responses. J Dent Res 94, 1035–1040.
Munasinghe, P.E., Riu, F., Dixit, P., Edamatsu, M., Saxena, P., Hamer, N.S. J., Galvin, I.F., Bunton, R.W., Lequeux, S., Jones, G., et al. (2016). Type-2 diabetes increases autophagy in the human heart through promotion of Beclin-1 mediated pathway. Int J Cardiol 202, 13–20.
Murdiastuti, K., Purwanti, N., Karabasil, M.R., Li, X., Yao, C., Akamatsu, T., Kanamori, N., and Hosoi, K. (2006). A naturally occurring point mutation in the rat *aquaporin 5* gene, influencing its protein production by and secretion of water from salivary glands. Am J Physiol Gastrointest Liver Physiol 291, G1081–G1088.
Proctor, G.B., and Carpenter, G.H. (2014). Salivary secretion: mechanism and neural regulation. Monogr Oral Sci 24, 14–29.
Riahi, Y., Wikstrom, J.D., Bachar-Wikstrom, E., Polin, N., Zucker, H., Lee, M.S., Quan, W., Haataja, L., Liu, M., Arvan, P., et al. (2016). Autophagy is a major regulator of beta cell insulin homeostasis. Diabetologia 59, 1480–1491.
Robinson, M.M., Dasari, S., Karakelides, H., Bergen 3rd, H.R., and Nair, K.S. (2016). Release of skeletal muscle peptide fragments identifies individual proteins degraded during insulin deprivation in type 1 diabetic humans and mice. Am J Physiol Endocrinol Metab 311, E628–E637.
Sinha, S., and Levine, B. (2008). The autophagy effector Beclin 1: a novel BH3-only protein. Oncogene 27 Suppl 1, S137–S148.
Sridhar, S., Botbol, Y., Macian, F., and Cuervo, A.M. (2012). Autophagy and disease: always two sides to a problem. J Pathol 226, 255–273.
Steinfeld, S., Cogan, E., King, L.S., Agre, P., Kiss, R., and Delporte, C. (2001). Abnormal distribution of aquaporin-5 water channel protein in salivary glands from Sjögren's syndrome patients. Lab Invest 81, 143–148.
Wang, X., Feng, Z., Li, J., Chen, L., and Tang, W. (2016). High glucose induces autophagy of MC3T3-E1 cells via ROS-AKT-mTOR axis. Mol Cell Endocrinol 429, 62–72.
Xiao, E., Mattos, M., Vieira, G.H.A., Chen, S., Corrêa, J.D., Wu, Y., Albiero, M.L., Bittinger, K., and Graves, D.T. (2017). Diabetes enhances IL-17 expression and alters the oral microbiome to increase its pathogenicity. Cell Host Microbe 22, 120–128.e4.
Xu, H., Shan, X.F., Cong, X., Yang, N.Y., Wu, L.L., Yu, G.Y., Zhang, Y., and Cai, Z.G. (2015). Pre- and post-synaptic effects of botulinum toxin a on submandibular glands. J Dent Res 94, 1454–1462.
Yang, J.S., Lu, C.C., Kuo, S.C., Hsu, Y.M., Tsai, S.C., Chen, S.Y., Chen, Y. T., Lin, Y.J., Huang, Y.C., Chen, C.J., et al. (2017). Autophagy and its link to type II diabetes mellitus. Biomedicine (Taipei) 7, 1–12.
Yao, F., Zhang, M., and Chen, L. (2016). 5′-Monophosphate-activated protein kinase (AMPK) improves autophagic activity in diabetes and diabetic complications. Acta Pharmaceut Sin B 6, 20–25.
Yin, Z., Pascual, C., and Klionsky, D.J. (2016). Autophagy: machinery and regulation. Microb Cell 3, 588–596.